Supporting Information

Nanostructured porous manganese carbonate spheres with capacitive effects on the high lithium storage capability

Wenpei Kang[a,b], Denis Yau Wai Yu[a,c], Wenyue Li[d,a,b], Zhenyu Zhang [a,b], Xia Yang[a,b], Tsz-Wai Ng[a,b], Rujia Zou[a,b] , Yongbing Tang[d,a]* , Wenjun Zhang[a,b] and Chun-Sing Lee[a,b]*

a Center of Super-Diamond and Advanced Films (COSDAF), City University of Hong Kong, Hong Kong SAR, People's Republic of China.

b Department of Physics and Materials Science, City University of Hong Kong, Hong Kong SAR, People's Republic of China.

c School of Energy and Environment, City University of Hong Kong, Hong Kong SAR, People's Republic of China.

d Functional Thin Films Research Center, Shenzhen Institutes of Advanced Technology, Chinese Academy of Sciences, People's Republic of China.

E-mail: tangyb@siat.ac.cn; apcslee@cityu.edu.hk; Tel: +852-34427826

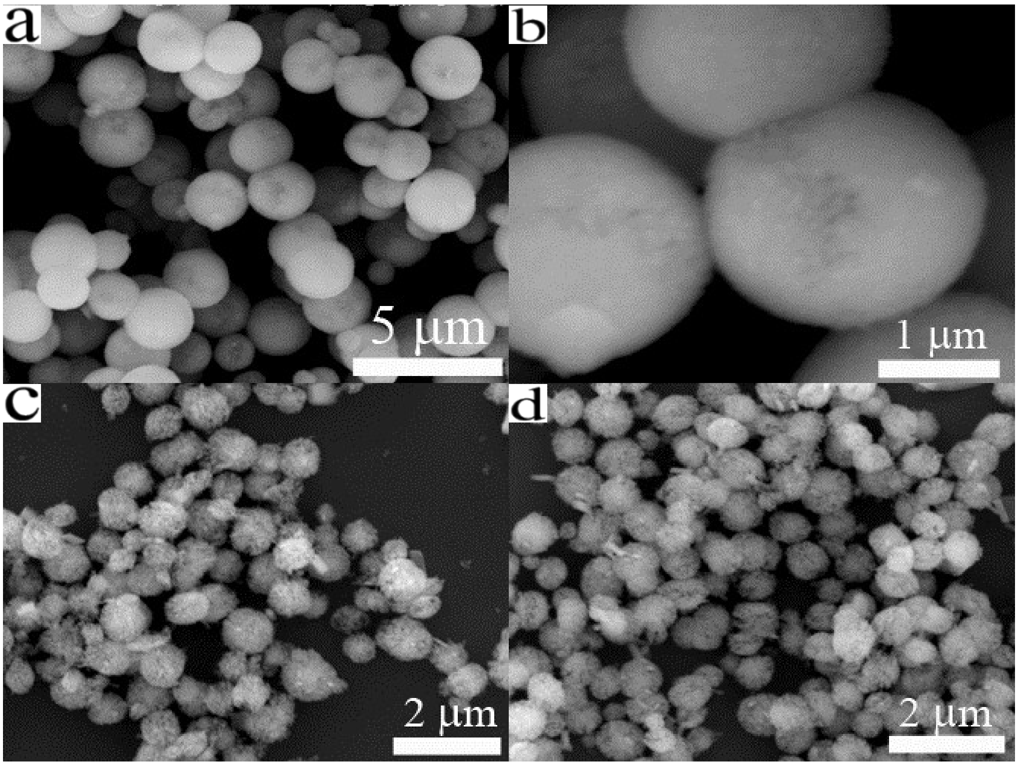

Fig. S1. SEM images of $MnCO_3$ obtained from (a, b) hydrothermal reaction; solvothermal reaction with (c) PVP and (d) acid ascorbate.

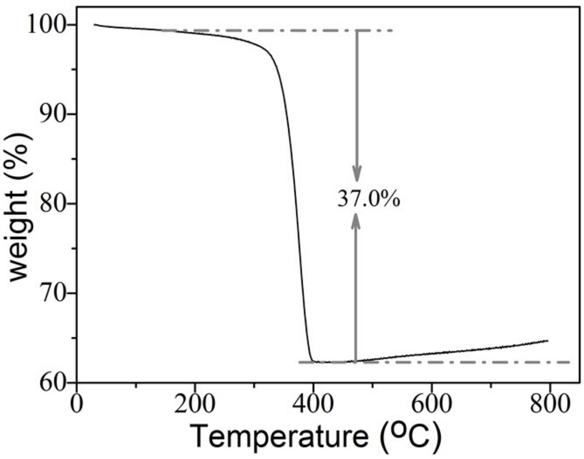

Fig. S2. Thermogravimetric measurement of p-$MnCO_3$ nanostructures. It indicates that $MnCO_3$ has a good thermal stability below 280°C.

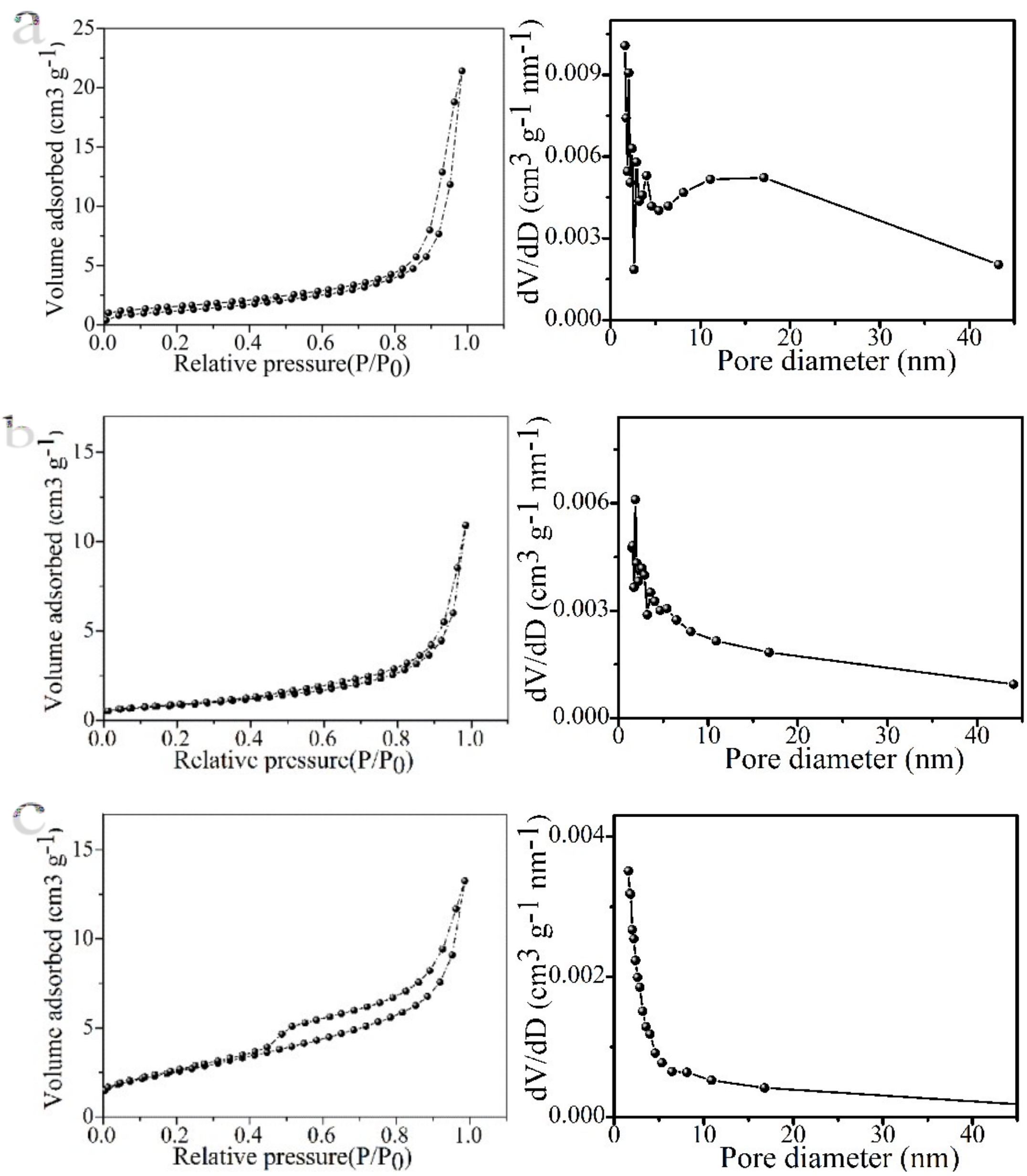

Fig. S3. N_2 adsorption–desorption isotherms curves (left) and pore size distribution (right) for (a) p-$MnCO_3$, (b) $MnCO_3$-R3 and (c) $MnCO_3$-R4. BET analysis of p-$MnCO_3$ gives a specific surface area of 25.4 m^2 g^{-1}, a pore volume of 0.188 cm^3 g^{-1} and average pore diameter of 3.2 nm. In comparison, the micro-size solid particle ($MnCO_3$-R3) gives a specific surface area of 17.2 m^2 g^{-1} and a pore volume of 0.09 cm^3 g^{-1} and average pore diameter of 3.7 nm. And the commercial sample ($MnCO_3$-R4) has BET areas of 11.3 m^2 g^{-1} and pore volume of 0.023 cm^3 g^{-1}.

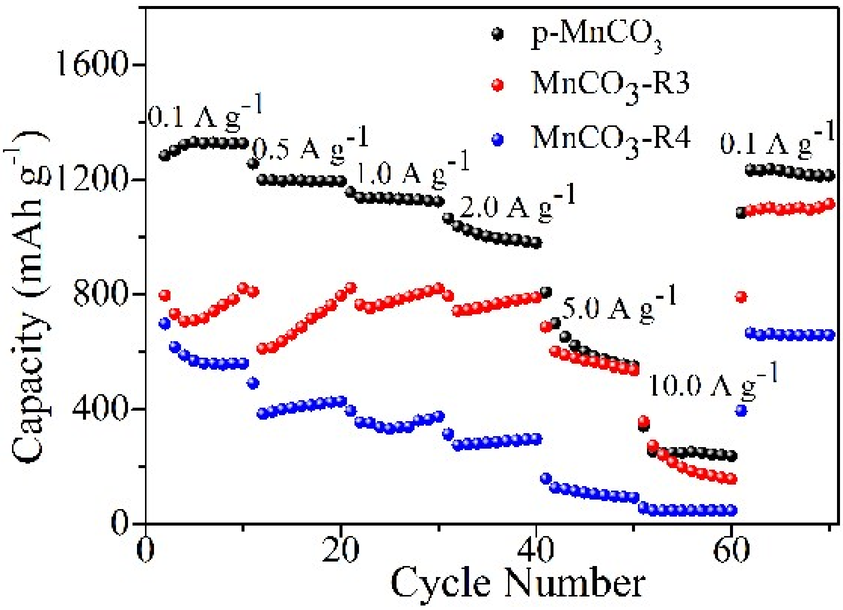

Fig. S4. Rate capabilities of different $MnCO_3$ samples.

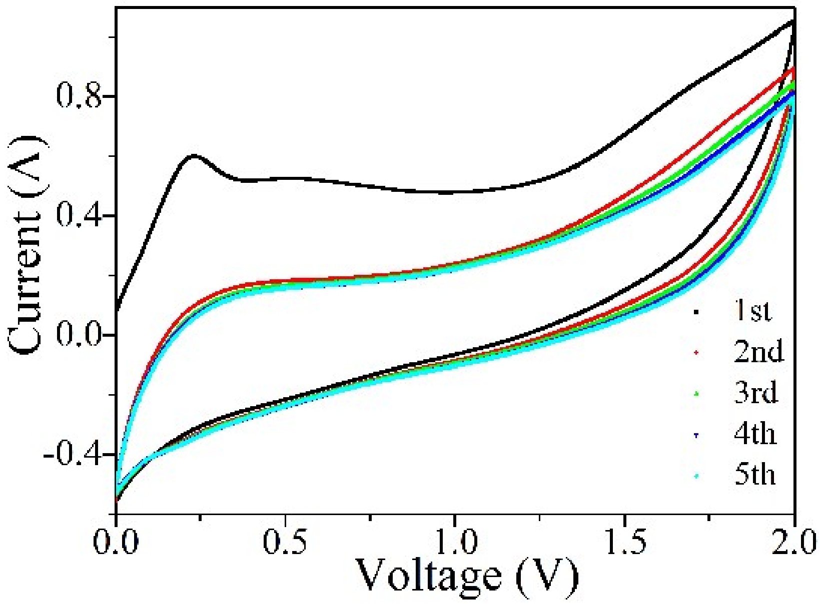

Fig. S5. CV curves for the symmetric supercapacitor with $MnCO_3$-$MnCO_3$ electrodes at a scan rate of 50 mV s^{-1}.

Table S1. A summary of the lithium storage capabilities of as-prepared porous $MnCO_3$ sphere in comparison with other high-performance anode materials reported in the literature.

Material	**Residual capacity (mAh g^{-1})**	**Current (mA g^{-1}) or C**	**Ref**
$MnCO_3$	**1049/200th cycle** **507/2000th cycle**	**1000** **5000**	**This Work**
Si/C	1160/1000th cycle	2100	*Nature Nanotech*, 2014, **9**,187
Si-PANi	550/4000th cycle	6000	*Nature Commun*, 2013, **4**, 1943
Si-CNT	~1300/100th cycle	800	*Nano Energy*, 2013, **2**, 138
Ge	1246/200th cycle	1C	*Chem. Mater.*, 2014, **26**, 5683
Ge	993/600th cycle 680/300th cycle	1C 2C	*Chem. Mater.*, 2014, **26**, 2172
Ge	888/1100th cycle	C/2	*Nano Lett.*, 2014, **14**, 716
SnO_2-PPy	448/100th cycle	0.1C	*Nano Energy*, 2014, **6**, 73
SnO_x /C	608/200th cycle	500	*Adv. Mater.*, 2014, **26**, 3943
Sn/C	1089/100th cycle 657/1000th cycle	0.2C 2C	*ACS Nano*, 2014, **8**, 1728

Table S2 A summary of the lithium storage capabilities of as-prepared porous $MnCO_3$ sphere in comparison with other oxysalt anode materials reported in the literature.

Material	**Shape**	**Residual capacity ($mAh\ g^{-1}$)**	**Current ($mA\ g^{-1}$) or C**	**Ref**
$MnCO_3$	**Porous sphere**	**1049/200th cycle** **507/2000th cycle**	**1000** **5000**	**This work**
$CoCO_3$/GNS	cubes	744/100th cycle 680/100th cycle	200 500	*Nano Energy*, 2013, **2**, 276
$CoCO_3$–polypyrrole	urchin-like structure	811.2/100th cycle 559/100th cycle	1000 5000	*J. Mater. Chem. A*, 2013, **1**, 11200
$CuC_2O_4xH_2O$	Cylinder-like structure	970/100th cycle 809/100th cycle	200 500	*J. Power Sources*, 2013, **238**, 203
FeC_2O_4	Elongated-shape	>400/75th cycle	2C	*Inorg. Chem.*, 2008, **47**, 10366
$MnCO_3$	Rhombohedron	>466/25th cycle	C/4	*Electrochem. Commun.* 2007, **9**, 1744
CoC_2O_4	Nanoribbon	<700/70th cycle	2C	*Chem. Mater.*, 2009, **21**, 1834
$FeCO_3$	Cubes	812/120th cycle	1000	*J. Power Sources*, 2014, **253**, 251
$FeCO_3$	Hollow Microspheres	710/200th cycle	200	*ACS Appl. Mater. Interfaces*, 2013, **5**, 11212